Bulletin of Earthquake Engineering
https://doi.org/10.1007/s10518-024-01874-4

ORIGINAL ARTICLE

Characteristics of torsional ground motions obtained for Turkey and their appraisal against Eurocode 8

Rafet Sisman[1,2] · **Ertugrul Taciroglu**[2]

Received: 7 January 2023 / Accepted: 5 February 2024
© The Author(s) 2024

Abstract
In current engineering practice, the torsional effects of ground motions are only considered implicitly through “accidental eccentricity coefficients". In seismic design codes, these coefficients account for not only the unintended (or uncertain) asymmetric distributions of structural mass and stiffness in the plan but also the torsional components of ground motions. The torsional effects may develop due to wave passage effects or the incoherency of translational ground motions along the foundation systems. While it is possible to obtain torsional components of ground motions directly from seismic records with modern instruments, such sensors are uncommon. Therefore, several numerical procedures have been proposed in the literature for estimating torsional components of ground motions from translational measurements. In this study, the Single Station Procedure (SSP)—based on the deconstruction of translational ground motions into body waves and the subsequent reconstruction of rotational ground motions—is employed to obtain torsional ground motions for seven different seismic events in Turkey. Additionally, the corresponding accidental eccentricity coefficients that can cause the same response modification with torsional ground motions are determined. First, a conventional procedure is utilized to obtain the corresponding accidental eccentricity coefficients. Various drawbacks of the conventional procedure, such as negative eccentricity coefficients, are addressed. Then, a relatively obscure definition of accidental eccentricity is revived to propose a novel procedure for determining accidental eccentricity coefficients. It is observed that the proposed procedure yields higher values for the accidental eccentricity coefficients than the conventional procedure. It also observed that the torsional spectrum provided in Eurocode 8 provisions requires higher eccentricity values than those implied by the recorded ground motions from Turkey.

Keywords Torsional ground motions · Accidental eccentricity · Torsional response spectrum · Response amplification due to torsion

Extended author information available on the last page of the article

Published online: 01 March 2024

1 Introduction

In engineering practice, ground motion components of seismic events are generally considered to be all translational. Typical measuring devices are capable of recording only the translational ground motions. However, rotational components of ground motions also exist and can be recorded, although this task requires nominally more expensive measuring devices. The rotational ground motions can be classified under two groups: namely, rocking and torsional motions. The rocking components of ground motions cause structures to rotate about a horizontal axis passing through the geometric center of the foundation. In contrast, the torsional component of ground motions causes structures to rotate about a vertical axis passing through the geometric center of the structure.

Ring Laser Gyroscopes (RLGs) make it possible to record rotational components of ground motions. However, their use is uncommon due to cost. On the other hand, various numerical approaches can be used for calculating (approximating) the rotational ground motions from given/recorded translational ground motions. The most common procedures for extracting rotational ground motions from translational ones are the Geodetic Method (GM) and the Single Station Procedure (SSP), which were proposed by Spudich et al. (1995) and Basu et al. (2012), respectively. It should be noted that these procedures yield only approximate rotational motions, and various modeling errors and measurement constraints limit their accuracy.

Seismic design requires an accurate definition of expected loads. In current practice, only the translational components of ground motions are used. The torsional effects are considered using simplified (and indirect) approaches. However, recent studies that examined the torsional components in detail indicated that their effects might have to be explicitly considered (Ghayamghamian et al. 2009; Ozsahin and Pekcan 2019, 2020a, b; Perron et al. 2018; Poudel et al. 2020; Dahmardeh etal. 2019).

The study by Mallet (1846) is likely the first scientific study in the modern sense that examined the effects of torsion in structures due to earthquakes. In this study, permanent deformations in chimneys and various monumental structures, such as obelisks, were attributed to the torsional effects, which were referred to as the “vorticose" effects of the seismic event. Despite the intervening 180 years, an isolated quantification of torsional seismic demands and their direct consideration in seismic design codes are yet to be achieved.

In literature (Gueguen and Astorga 2021), earthquake-induced torsion in buildings has been cited as being due to three reasons: (i) load-carrying elements or structural masses can be located asymmetrically in the plan, (ii) asymmetric stiffness or mass distributions due to imperfect construction, (iii) torsional ground motions caused by seismic wave passage (i.e., seismic waves reaching different points of the foundation at different times) or incoherent translational ground motion (variation of seismic waves at different points of the foundation due to reflection and refraction). Since most, if not all, of the current design codes allow inelastic response, a fourth possibility should also be considered, wherein structural damage occurs asymmetrically, causing a damage-induced torsional eccentricity. While the first two and the fourth of the aforementioned reasons can be considered directly in the design procedures, the third case cannot be (is not) directly considered in current practice. The effects of torsional ground motions are currently lumped together with the provisions for imperfect/uncertain construction geometries and are approximated through the so-called *accidental eccentricity coefficients*.

The intentional/known asymmetric distributions of mass and stiffness are referred to as *static eccentricity*. Static eccentricity can be explicitly considered both in dynamic analyses of 3D numerical models and in quasi-static methods such as the Equivalent Lateral Force (ELF) approach. However, studies have shown that the structural responses obtained from dynamic analyses with 3D numerical models are larger than those obtained from quasi-static methods (Housner and Outinen 1958). Therefore, it is recommended that the static eccentricity values are scaled up by a factor of 1.5 in Eurocode (1996) in the ELF approach.

Considering a linear-elastic structure without any static eccentricity, it can be said that the torsional effects will result only from the torsional component of the ground motion (under simultaneous unidirectional lateral and torsional ground excitations). This situation is only theoretically possible, since there may always be a difference between design and construction, leading to physical eccentricities. However, numerical models without any static eccentricity have been frequently used for investigating/evaluating the adequacy of accidental eccentricity coefficients proposed in earthquake codes (Ghayamghamian and Nouri 2007; Ghayamghamian et al. 2009; Basu et al. 2014). Studies (Ghayamghamian et al. 2009; Anagnostopoulos et al. 2015; Rutenberg 1992) have suggested that the accidental eccentricity coefficient given as 0.05 or 0.10 in earthquake codes should be revised, for example, to 0.60 for structures with periods of less than 0.30 s for the translational mode (low-rise rigid structures) (Ghayamghamian et al. 2009).

In Eurocode (1996), rotational response spectra are provided to consider the effects of the torsional components of ground motions during the design of towers and masts. The torsional design spectrum is obtained from the horizontal elastic design spectrum, and is a function of the fundamental period corresponding to the translational mode of vibration (see Part 6 of Eurocode (1996)). The absence of any dynamical properties of the structure related to the torsional mode is considered to be the biggest shortcoming of this approach (Gueguen and Astorga 2021).

The primary objective of this study is to extract torsional ground motions from translational accelerograms that were recorded during various seismic events that occurred in Turkey. Located in one of the most seismically active regions of the world, Turkey's primary source of seismicity is the North Anatolian Fault (NAF) line, which cuts across the entire country. However, the East Anatolian Fault (EAF) line and the West Anatolian Fault (WAF) zone can also produce destructive earthquakes. The seismic design guidelines and regulations in Turkey are being continuously updated (with the latest revisions published in 2018) to improve the country's seismic resilience. However, as is the case for most other seismic guidelines, the torsional ground motion time histories are not considered directly in the design calculations.

The secondary objective of the present study is to investigate the potential effects of torsional ground motions on structures using these extracted torsional motions. In the literature, the effects of torsional ground motions are generally addressed in terms of implied accidental eccentricity and displacement response amplifications. Therefore, addressing the accidental eccentricity coefficients that correspond to the torsional ground motions for Turkey gives us the ability to evaluate code-recommended (Turkish Building and Earthquake Code-2018, (TBEC 2018)) accidental eccentricity coefficients. Determination of corresponding/implied accidental eccentricity values can be achieved in several ways. First, the conventional approach—which is based on shifting the center of mass for determining implied accidental eccentricity values—is employed. Next, a *novel procedure* is proposed for determining the accidental eccentricity values corresponding to torsional

ground motions, which avoids the shortcomings of the conventional approach, as will be elaborated in detail.

2 Methodology

The accidental eccentricity values corresponding to a specific torsional ground motion can be obtained through two different approaches. In the conventional procedure, which is also employed in this study, accidental eccentricity values are determined by calculating the required shift of the center of mass that yields the same displacement amplification with the consideration of the torsional ground motion. In a relatively new procedure, accidental eccentricity values are obtained by calculating the required “arm" length to convert translational ground motion to a representative torsional ground motion that would yield the same displacement amplification with the consideration of the actual torsional excitation (Basu et al. 2014).

The accidental eccentricity values corresponding to torsional ground motions are also referred to as implied accidental eccentricity. There are two dynamic systems/load cases considered in this study to determine the implied accidental eccentricity values: (i) a dynamic system with an unknown accidental eccentricity, excited by unidirectional translational motions only and (ii) a dynamic system without accidental eccentricity, excited by both translational and torsional motions simultaneously. Our purpose is to determine the unknown accidental eccentricity value for case (i) that would yield the same peak response as case (ii). Therefore, the implied (corresponding) accidental eccentricity coefficients depend on the considered ground motions.

A two-dimensional dynamic system is employed in this study for the calculation of accidental eccentricity values that can represent the effects of torsional ground motions. The dynamic system depicted in Fig. 1 consists of a rigid slab supported by four springs. Eccentricity is considered only along the *X*-direction, and the springs in the *X*-direction have equal stiffness values ($k_{x1} = k_{x2}$). The slab dimensions are a and b in Y and X directions, respectively. In the figure, *CM* represents the center of mass, while *CS* represents the center of stiffness. The lateral distance between *CM* and *CS* is the static (inherent) eccentricity and is denoted by e. On the other hand, translational excitation is only considered in the *Y*-direction since the system is eccentric only along the *X*-direction. Thus, the system has only two degrees of freedom, which correspond to the translational and

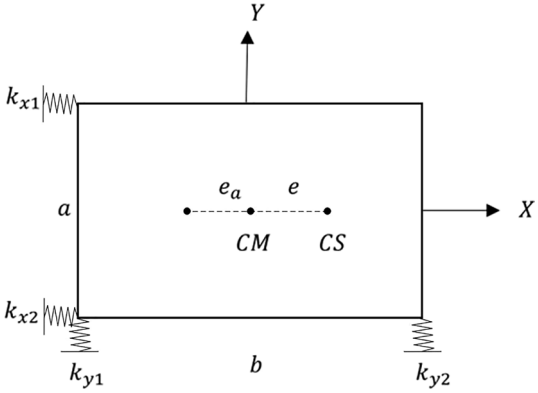

Fig. 1 Schematic representation of the dynamic system in question

torsional vibration modes. It must be noted here that the torsional mode of vibration represents the rotations about the vertical axis passing through the center of mass.

The parameters that are required to define such a dynamic system, shown in Fig. 1, are the damping ratio (ξ), translational angular frequency ω_y, torsional angular frequency ω_θ, dimensions of the slab (a and b) and static eccentricity (e). An aspect ratio (γ) is defined as the ratio of a to b to have simplicity in the equations. On the other hand, the torsional angular frequency can be represented as a function of translational angular frequency as $\omega_\theta = \Omega.\omega_y$ for more concise equations. Basically, both the translational and torsional stiffnesses of such a dynamic system depend on the individual stiffnesses of the springs. Thus, either torsional stiffness or translational stiffness can be represented as a function of the other. This type of parameterization was also employed in similar studies (Ghayamghamian et al. 2009; Dahmardeh etal. 2019). The inherent eccentricity can also be given as a fraction of the slab dimension along the considered direction as $e = \beta.b$. Thus, the parameters that define a dynamic system for numerical analyses are ω_y, b, Ω, γ, β, and ξ. The matrix representation of the equations of motion for the system is given in Eq. 1.

$$\begin{bmatrix} m & 0 \\ 0 & m \end{bmatrix} \cdot \begin{Bmatrix} \ddot{u}_y \\ r.\ddot{u}_\theta \end{Bmatrix} + C. \begin{Bmatrix} \dot{u}_y \\ r.\dot{u}_\theta \end{Bmatrix} + \begin{bmatrix} K_y & K_y.e/r \\ K_y.e/r & K_\theta/r^2 \end{bmatrix} \cdot \begin{Bmatrix} u_y \\ r.u_\theta \end{Bmatrix} = - \begin{bmatrix} m & 0 \\ 0 & m \end{bmatrix} \cdot \begin{Bmatrix} \ddot{u}_{gy} \\ \ddot{u}_{g\theta} \end{Bmatrix} \quad (1)$$

In Eq. 1, m is the mass associated with translational mode, r is the radius of gyration for the slab, C is the damping matrix that is obtained by using Rayleigh damping coefficients, and K_y and K_θ are the translational and torsional stiffness values. The Rayleigh damping coefficients are calculated in such that the first two fundamental modes (with frequencies ω_y and ω_θ) have 5% damping. The input acceleration histories are depicted as $\ddot{u}_{gy}$ and $\ddot{u}_{g\theta}$, which correspond to the translational acceleration history along the Y-direction and the torsional acceleration history around the vertical axis passing through the center of mass. The output displacement and rotation histories are depicted as u_y and u_θ, respectively, and dotted representations correspond to their time derivatives. Assuming an arbitrary value for the total mass of the dynamic system, the other terms of the equations of motion can be derived as shown in Eq. 2.

$$\begin{aligned} m_\theta &= mr^2 \\ K_{\theta S} &= m_\theta \omega_\theta^2 \\ K_y &= m\omega_y^2 \\ K_\theta &= \frac{b^2}{4}(k_{y1} + k_{y2}) + \frac{a^2}{4}.(k_{x1} + k_{x2}) \\ K_{\theta S} &= K_\theta - K_y e^2 \\ K_y &= k_{y1} + k_{y2} \\ K_x &= k_{x1} + k_{x2} \\ e &= \frac{-k_{y1}\frac{b}{2} + k_{y2}\frac{b}{2}}{K_y} \end{aligned} \quad (2)$$

In the above equations, $K_{\theta S}$ is the torsional stiffness of the system with respect to the center of stiffness, while K_θ is the torsional stiffness of the system with respect to the center of mass. In the case of zero static eccentricity ($e = 0$), these two values become identical. As stated before, the spring stiffness values along the X-direction are identical. Thus, the

above equations represent three equations with three unknowns. Further manipulation of the equations yields a lower limit for the parameter Ω as given in Eq. 3.

$$\begin{aligned}
\omega_\theta^2 mr^2 &= K_y\left(\frac{b^2}{4}-e^2\right)+K_x\left(\frac{a^2}{4}\right)\\
\Omega^2 &= \frac{K_y}{\omega_y^2.m.r^2}\left(\frac{b^2}{4}-e^2\right)+\frac{K_x}{\omega_y^2 mr^2}.\left(\frac{a^2}{4}\right)\\
\Omega^2 &= \left(\frac{b^2}{4r^2}-\frac{e^2}{r^2}\right)+\frac{K_x}{K_y}\left(\frac{a^2}{4r^2}\right)\\
\Omega^2 &= \frac{1}{r^2}\left(\frac{b^2}{4}-e^2\right)+\frac{K_x}{K_y}\left(\frac{a^2}{4}\right)\\
K_x &> 0 \qquad K_y > 0\\
\Omega^2 &> \frac{1}{r^2}\left(\frac{b^2}{4}-e^2\right)\\
r &= b\sqrt{\frac{1+\gamma^2}{12}}\\
\Omega &> \sqrt{\frac{3-12\beta^2}{1+\gamma^2}}
\end{aligned} \tag{3}$$

This limitation must be satisfied to be able to define a system by using the aforementioned parameters. Otherwise, the stiffness values associated with the springs along the *X*-direction would be negative, which is physically unreasonable. To have reasonable stiffness values in the *X*-direction, the ratio between torsional angular frequency and translational angular frequency must satisfy the limit given in Eq. 3. The limit vanishes to 0 as the static eccentricity coefficient (β) approaches 0.5, which corresponds to a slab-column system with all stiffness located at one edge. In this study, reasonable values of the system parameters are employed for the numerical analyses.

2.1 Torsional ground motions

In this study, the Single Station Procedure (SSP) is utilized for obtaining torsional ground motions from translational ground motions. Seven different seismic events that occurred in various regions of Turkey are selected for the numerical analyses. Since the SSP is applicable to cases where source-to-station distances are below 20 km, the seismic events are chosen accordingly. The seismic events and recording stations are shown on the map in Fig. 2. The properties of the earthquakes and recording stations are listed in Table 1. As seen from the table, the maximum epicentral distance is 15.24 km. The acceleration histories, earthquake, and station properties for the considered events are obtained from the AFAD (AFAD 2022) website. The magnitudes (M_w) of seismic events vary between 5.8 and 7.6, while the focal depths vary between 4.3 km and 15.9 km.

Since all the numerical analyses are linear elastic and we are interested in response amplifications, rather than the response, the acceleration histories are not scaled. As stated previously, the torsional motions are derived from the translational ones; if the translational motions were scaled, then the torsional motions would also be (inherently) scaled in the same way. Thus, the response amplification values would be the same. The acceleration

Table 1 Event and station information for the considered recordings

Event name	Date	Event ID	M_w	Focal depth (km)	Station ID	$V_{S,30}$ (m/s)	$V_{P,30}$ (m/s)	Epi. Dist
Izmit (Kocaeli)	09/13/1999	248095	5.8	4.3	4101	818	2486	13.79
Golyaka (Duzce)	11/23/2022	536492	5.9	6.81	8101	282	1210	10.67
Bozkurt (Denizli)	08/08/2019	444581	6.0	10.92	2005	396	1115	7.96
Orta (Cankiri)	06/06/2000	250446	6.0	10.5	1801	347	2019	15.24
Merkez (Bingol)	05/01/2003	236848	6.3	6.0	1201	526	1409	11.79
Duzce (Bolu)	11/12/1999	246572	7.1	11.0	8101	282	1210	5.27
Golcuk (Izmit)	08/17/1999	247730	7.6	15.9	4101	818	2486	3.40



Fig. 2 Earthquake and station locations

histories in three translational directions are plotted in Fig. 3. As seen from the figure, the horizontal PGAs vary between 0.0634g and 0.5229g. The response spectra corresponding to the geometric mean of the horizontal acceleration histories are given in Fig. 4 together with the response spectra of obtained torsional motions. The event IDs corresponding to each plot are also written on each graph. As seen from the figure, for the events recorded at soft soil sites, translational spectral ordinates at larger periods are higher when compared to the events recorded at stiff soil sites. On the other hand, torsional response spectra do not have significant amplitudes for periods above 1.0 s, regardless of the site/soil conditions. This was also previously shown by Basu et al. (2012) and observed by Yin et al. (2016). However, we can still evaluate dynamic systems with translational periods above 1.0 s, since the parameter Ω (we used values larger than 1.0) will yield torsional periods smaller than translational periods.

A MATLAB code for the SSP procedure was previously developed by Basu et al. (2012). The SSP is based on deconstructing the translational ground motions into body waves and the reconstruction of rotational ground motions by using these body waves. Any contribution from the surface waves to rotational ground motions is not considered in the SSP. There is also a Python twin of this MATLAB code, dubbed *ExRGM* (can be

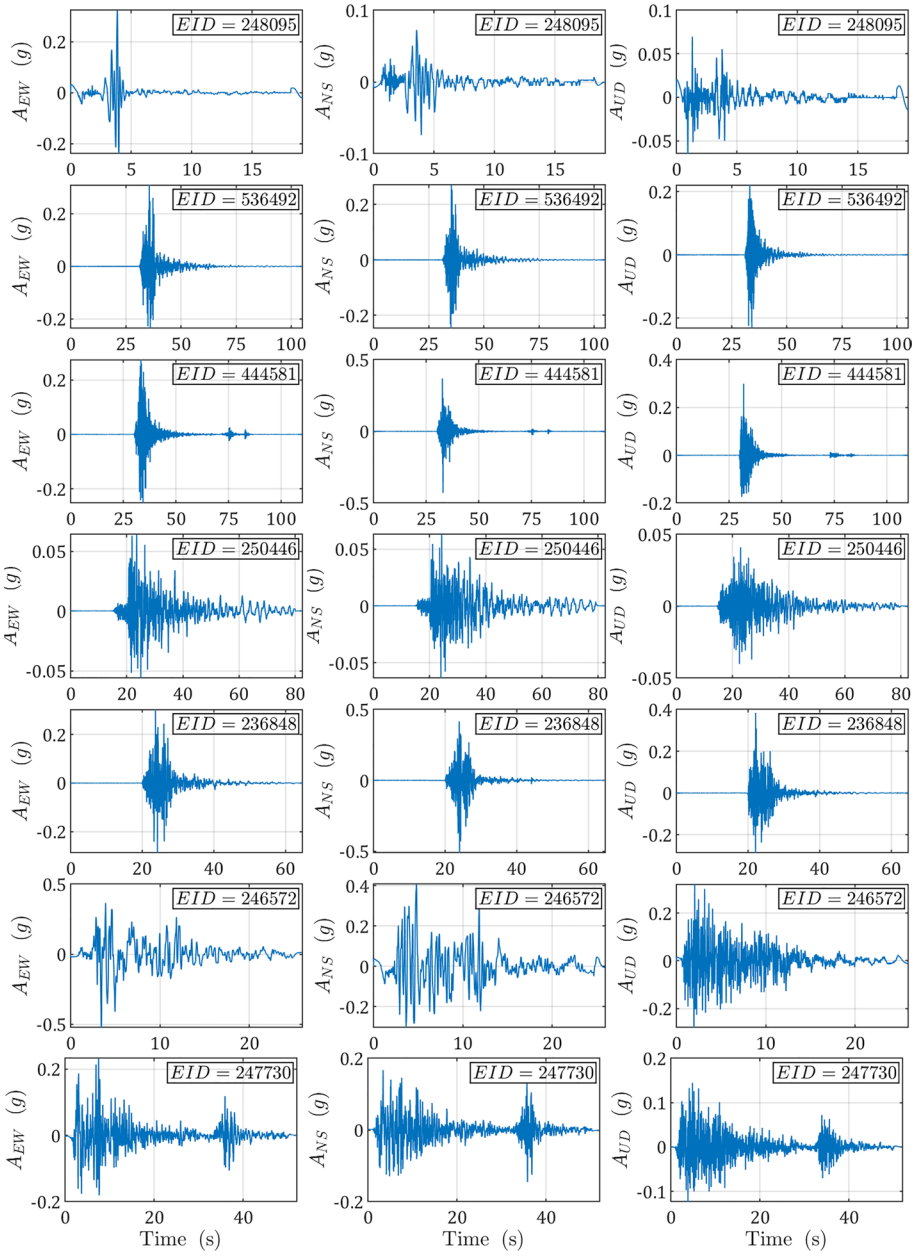

Fig. 3 Translational acceleration histories for seven different seismic events

requested from the authors), which the authors of the present paper developed, which uses the event properties given in Table 1 together with the source and station location information and produces the torsional acceleration histories. The obtained torsional

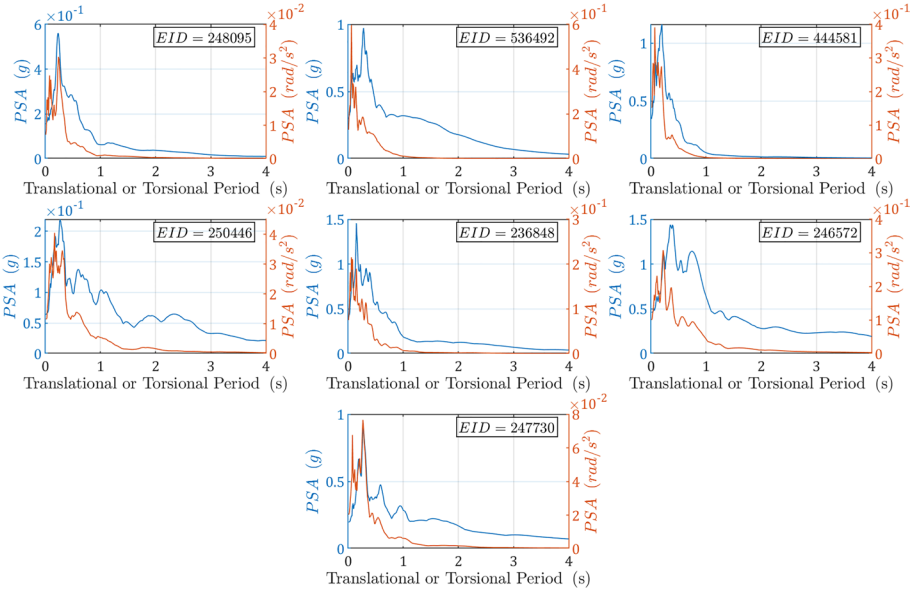

Fig. 4 Translational response spectra (geometric mean) and obtained torsional response spectra for considered seismic events

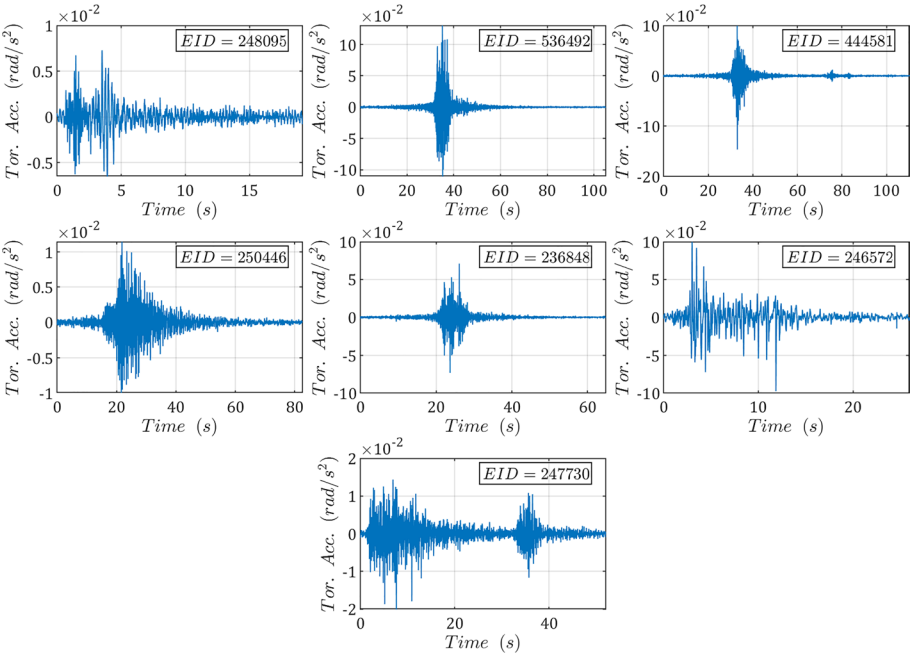

Fig. 5 Torsional acceleration histories extracted from the translational acceleration histories

acceleration histories at each station are plotted in Fig. 5. As seen from the figure, the torsional acceleration values vary between 0.0073 rad/s^2 and 0.1462 rad/s^2.

2.2 Determination of accidental eccentricity coefficients

As per the conventional procedure, there are three cases to investigate: (i) translational ground motion excitation only, (ii) simultaneous excitation of torsional and translational ground motions, (iii) translational ground motion excitation with consideration of accidental eccentricity. The peak displacement responses at $x = -r$ (w.r.t. the center of mass) in cases (ii) and (iii) will differ from the displacement response in case (i). The aim of the conventional procedure is to determine the required accidental eccentricity coefficient for case (iii) to have the same displacement response change as case (ii). In this manner, the peak displacement response obtained by considering simultaneous excitation of torsional and translational ground motions (i.e., case (ii)) can be derived as given in Eq. 4. Similarly, the peak displacement response corresponding to the consideration of translational excitation only (i.e., case (i)) can be derived as given in Eq. 5. The change in the displacement response can be obtained as a function of the system parameters by dividing $U^{tt}_{x=-r}$ by $U^{t}_{x=-r}$. The change in the peak displacement is given in Eq. 6. It must be noted that the considered base shear is the same for all cases since the lateral displacement response due to translational excitation will always be the same.

$$U^{tt}_{x=-r} = \frac{V}{K_y} + \frac{V\left(e + e_a\right)(e + r)}{K_{\theta S}} \tag{4}$$

$$U^{t}_{x=-r} = \frac{V}{K_y} + \frac{V\, e\,(e + r)}{K_{\theta S}} \tag{5}$$

$$\hat{U}_{x=-r} = \frac{U^{tt}_{x=-r}}{U^{t}_{x=-r}} = \frac{V\,K_{\theta S} + V\,K_y\left(e + e_a\right)(e + r)}{V\,K_{\theta S} + V\,K_y\, e\,(e + r)} \tag{6}$$

The required accidental eccentricity coefficient that yields the same displacement response change with consideration of torsional ground motions can be obtained by manipulating Eq. 6. The relationship for the corresponding accidental eccentricity coefficient is given in Eq. 7 as a function of four system parameters and displacement amplification values. As seen from Eq. 7, the accidental eccentricity corresponding to the consideration of torsional excitation is independent of the base shear (Ghayamghamian et al. 2009). In Eq. 7, the accidental eccentricity appears as divided by b. Thus, it becomes compatible with the accidental eccentricity coefficients provided in seismic codes.

$$\frac{e_a}{b} = \left[\frac{r.\Omega^2}{(e + r)} + \frac{e}{r}\right]\frac{r}{b}\left(\hat{U}_{x=-r} - 1\right) \tag{7}$$

As stated before, there are seven different seismic events used for numerical analyses. For each seismic event, there are two horizontal acceleration histories and one torsional acceleration history, which means we have 14 different cases to consider in numerical analyses. In the utilized procedure, the peak displacement value at $x = -r$ is determined by simultaneous consideration of torsional and translational ground motions. Then, the peak

displacement value at the same location under only translational excitation is calculated. The ratio of these two peak displacement values is obtained for 14 cases and averaged. In the end, the accidental eccentricity values for various system parameter combinations are calculated using Eq. 7. The spectra of the obtained accidental eccentricity coefficients are presented in the next section.

3 Effects of torsional ground motions

The torsional excitation effects are presented herewith, shedding light on the critical parameters. The system parameters defined in the previous chapter are used for the parametric investigation of the torsional excitation effects. In the parametric study, the width of the slab (b) varies as 20 m, 40 m, and 60 m, while the aspect ratio (γ) varies as 1 and 1.5. The static eccentricity parameter (β) varies as 0, 0.1, 0.2, and 0.3. And the torsional to translational frequency ratio parameter (Ω) is given the values of 1.25, 1.5, and 2.

Two measures for torsional excitation are presented in this paper, (i) the displacement amplification due to torsional excitation and (ii) the corresponding accidental eccentricity. Since we have seven different seismic events and two horizontal acceleration components for each, we have 14 translational ground motions. However, since the SSP yields a single torsional ground motion per station, we have seven torsional ground motions in total. Combining each translational ground motion with the corresponding torsional ground motion, we have 14 different input motion cases to be averaged. Namely, each displacement amplification or accidental eccentricity value represents the mean of 14 cases. Figures 6, 7 and 8 show the displacement amplification values. Values of the parameters for each case are given in the title of the corresponding plot. In each figure, there are six plots corresponding to different values of γ and Ω. And the plots are located in such a way that the Ω values increase from left to right while the γ values increase from top to bottom.

As seen from Figs. 6, 7 and 8, the displacement amplification values increase as the width of the slab increases. In fact, this increase is caused by the change of location where the displacement responses are measured. As stated before, the peak displacement

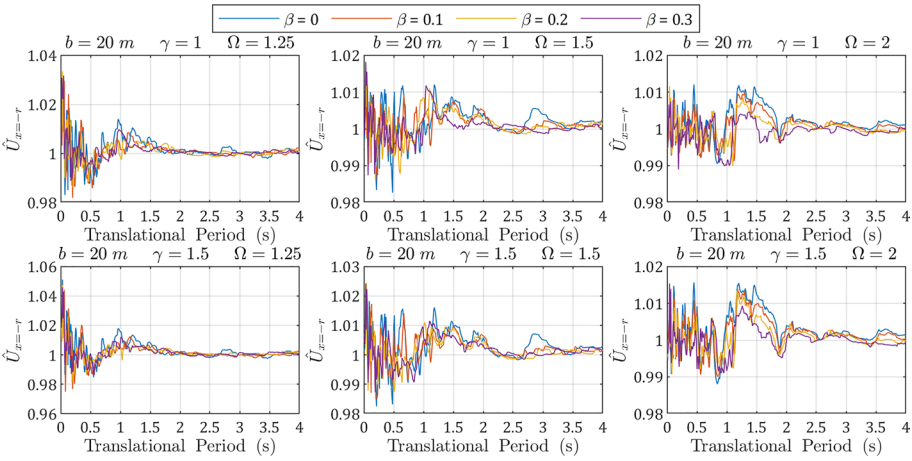

Fig. 6 Displacement amplifications due to torsional excitation for cases with b = 20 m

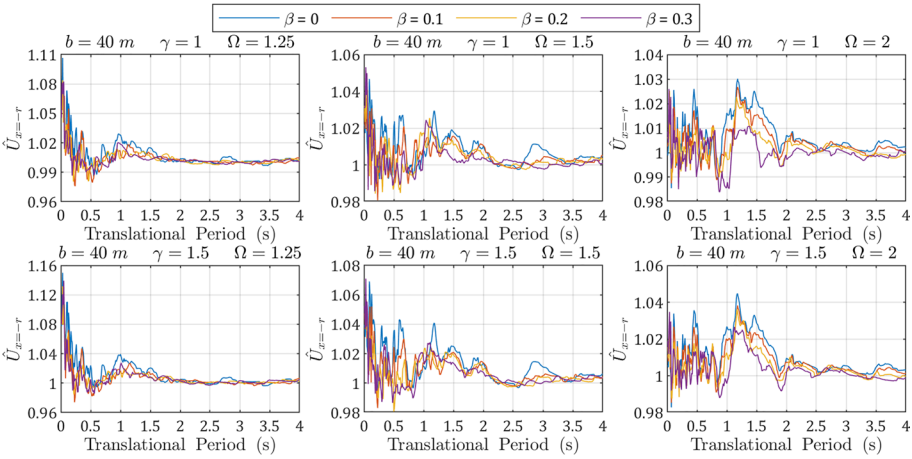

Fig. 7 Displacement amplifications due to torsional excitation for cases with b = 40 m

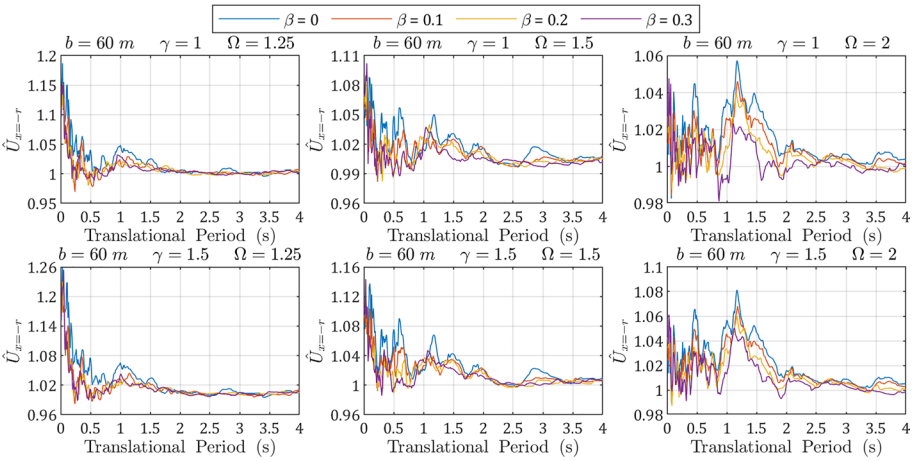

Fig. 8 Displacement amplifications due to torsional excitation for cases with b = 60 m

responses were calculated at a distance (r) from the center of mass. Since r is a linear function of b, any increase in b causes a direct increase in r. Therefore, as the point of measurement gets farther away from the center of mass, the contribution of torsional response to translational response increases. Thus, the amplification due to torsional excitation increases with parameter b. Similarly, the displacement amplification values slightly increase with increasing aspect ratio values. As seen from the figures, the plots on the bottom strip have larger ordinate values than those on the top strip. This is also related to the change of measurement location since r is also a function of γ.

On the other hand, any increase in Ω values causes an overall decrease in the displacement amplification values. Variation of Ω represents the change in dynamic characteristics related to the torsional mode of structure. Larger Ω values correspond to torsionally stiff structures, while smaller values correspond to torsionally flexible structures. Increasing

torsional stiffness causes a decrease in the contribution of the torsional mode to total response. However, variation of Ω causes increases in the displacement amplification values for the specific period ranges depending on the value of Ω. Each Ω value causes the frequency of the torsional mode to coincide with another harmonic of the torsional ground motion. If that frequency corresponds to a larger amplitude in the torsional ground motion response spectrum, the displacement response increases, and vice versa. For the torsional response spectra, the period ranges between 0.01 and 1.0 s have the largest spectral amplitudes. Therefore, for each Ω value, oscillators with approximate torsional frequencies yield response amplifications.

The effect of static eccentricity parameter β on the displacement amplification values cannot be remarked on for smaller periods. However, for the larger periods, increasing β values causes a decrease in the displacement amplification values. An increase in the parameter β increases the contribution of lateral stiffness to torsional stiffness. Thus, the total displacement response decreases with increasing β values. This property of static eccentricity is a useful finding, as it means omitting β yields conservative accidental eccentricity coefficients.

The accidental eccentricity values for various cases are shown in the Figs 9, 10 and 11. The effects of parameters on the displacement amplification values are also valid for the corresponding accidental eccentricity values. Namely, the accidental eccentricity values increase with increasing b and γ values, while they decrease with increasing β values. The effect of Ω is, again, period-dependent, although increasing values of Ω cause an overall decrease in the accidental eccentricity values.

The largest accidental eccentricity is obtained for the case with $b = 60m$, $\gamma = 1.5$, $\Omega = 1.25$, and $\beta = 0$ as 0.2104. However, it must be noted that the plotted values are averaged values obtained for two horizontal components of seven different ground motions. The real maximum value for accidental eccentricities of all cases is 1.6842, which is physically meaningless but implies the importance of considering torsional ground motions. Therefore, it can be said that the use of code-recommended accidental eccentricity coefficients (0.05 in (TBEC 2018) and 0.05/0.10 in (Eurocode 1996)) to account for torsional ground motion effects could be unconservative in some cases. The code-recommended

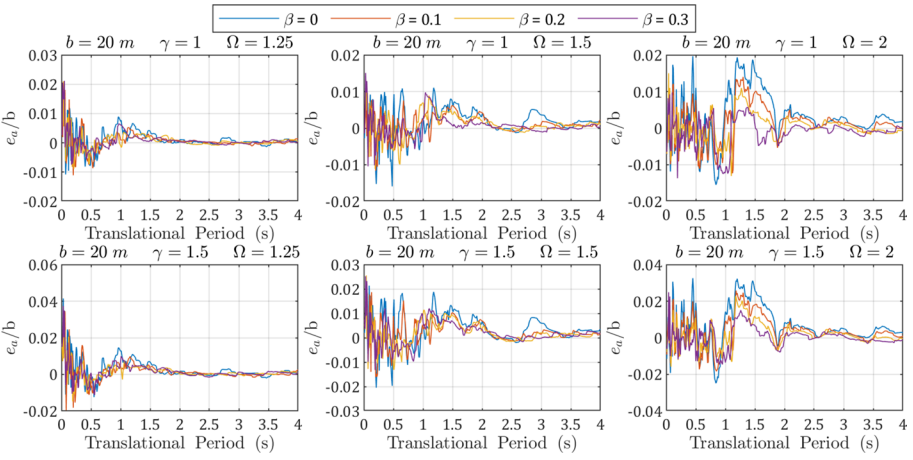

Fig. 9 Accidental eccentricity values for cases with b = 20 m

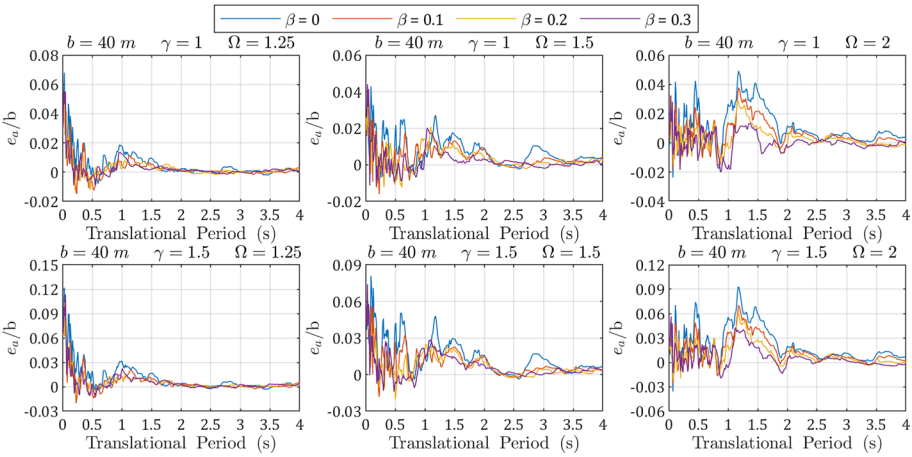

Fig. 10 Accidental eccentricity values for cases with b = 40 m

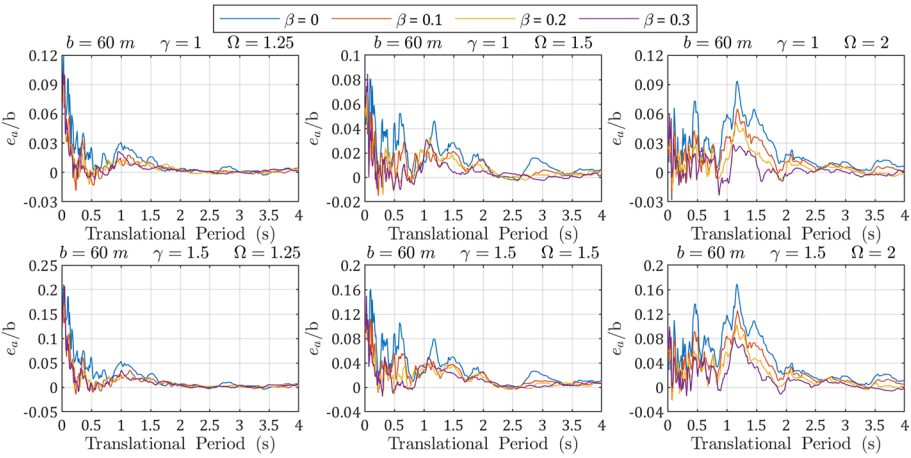

Fig. 11 Accidental eccentricity values for cases with b = 60 m

values are undoubtedly useful and they are meant to aid in the safe design of many buildings and it appears that slight revisions could achieve better conservatism. A possible solution could be defining an accidental eccentricity spectrum. However, this requires a huge torsional ground motion dataset, which is not currently available.

On the other hand, the corresponding accidental eccentricity coefficients are highly dependent on the ground motion time histories. For instance, if the peak times of translational and torsional acceleration histories coincide—assuming both have the same sign, then it would yield a larger corresponding accidental eccentricity coefficient. For the same example, if the peaks have opposite signs, then it would yield a smaller corresponding accidental eccentricity coefficient. Therefore, a novel definition of accidental eccentricity seems to be required. In the next section, a novel accidental eccentricity definition is proposed.

4 A novel accidental eccentricity definition

In the previous section, it is shown that the current procedures for obtaining accidental eccentricity that accounts for torsional ground motions are inaccurate. The maximum of the presented accidental eccentricity values is 0.21, while the actual maximum is 1.68. And in some cases, negative valued accidental eccentricity happens to be required to account for torsional ground motions. However, the purpose of accidental eccentricity is to account for uncertainties, and conservative values should be preferred. Therefore, a novel definition of accidental eccentricity is proposed in this paper.

In the previous section, it is shown that different values of b and γ correspond to measuring the displacement response at different locations. Instead of the lateral displacement that can occur due to torsional excitation, we recommend using torsional rotation itself as a measure of its effect on the structure. According to the proposed definition, accidental eccentricity is defined as the "arm" length that is required for the translational seismic force to create the maximum rotation that the torsional ground motions can cause. Actually, this definition is merely a slightly different expression of the accidental eccentricity definition given by Rutenberg and Heidebrecht (1985). In that study, accidental eccentricity is defined as the ratio of spectral torque and spectral base shear. However, the author did not expand the definition to include any parameters that correspond to γ and Ω parameters.

To be able to use the novel definition, the maximum (spectral) values of the torsional and translational responses need to be known. Using the *ExRGM* code, one can obtain the torsional ground motions for previously recorded seismic events. Therefore both torsional and translational response spectra can be obtained. By using these response spectra, accidental eccentricity values corresponding to each dynamic system can be obtained as given in Eq. 8.

$$\begin{aligned} \frac{PSA^{tra} m e_a}{m r^2 \omega_\theta^2} &= SD^{tor} \\ e_a &= \frac{SD^{tor}\left(T_y/\Omega\right)}{PSA^{tra}\left(T_y\right)} r^2 \Omega^2 . \omega_y^2 \\ e_a &= \frac{SD^{tor}\left(T_y/\Omega\right)}{PSA^{tra}\left(T_y\right)} \frac{b^2\left(1+\gamma^2\right)}{12} \Omega^2 \omega_y^2 \\ \frac{e_a}{b} &= \frac{SD^{tor}\left(T_y/\Omega\right)}{PSA^{tra}\left(T_y\right)} \frac{b.\left(1+\gamma^2\right)}{12} \Omega^2 \omega_y^2 \end{aligned} \tag{8}$$

In Eq. 8, PSA^{tra} represents the pseudo-spectral acceleration obtained using translational ground motions while SD^{tor} corresponds to the spectral rotations obtained using torsional ground motions. As seen in Eq. 8, SD^{tor} is a function of the torsional period, while PSA^{tra} is a function of the translational period. The other terms are previously defined system parameters. It must be noted that the static eccentricity parameter does not appear in this equation, and the accidental eccentricity values can only be determined for zero static eccentricity. This simplification may be thought of a cause for inaccuracies. However, as explained in the previous section, lower values of static eccentricity yield larger accidental eccentricity values. Thus, the omission of static eccentricity in the calculations results in conservative accidental eccentricity coefficients.

The accidental eccentricity coefficients obtained by using the proposed method are given in Fig. 12. The spectral presentation of the accidental eccentricity values is given for 18 cases with varying b, γ, and Ω values. Remarkably, the shape of the spectral representation varies only with Ω while b and γ parameters just scale the ordinate values. This is because the parameters b and γ have nothing to do with the dynamic characteristics of the system. The two-DOF system is defined by only two fundamental periods and a damping ratio, which is set to be 5% for all cases. This property of having a standard spectral shape may be exploited to recommend accidental eccentricity spectra. However, such a task would require a large seismic event catalog.

As seen from Fig. 12, the accidental eccentricity values are always positive, which means torsional ground motions always cause detrimental effects. In the previous section, it was stated that the torsional ground motions might be beneficial in terms of peak displacement response depending on the torsional ground motion time history. However, for such an uncertain phenomenon, being on the conservative side should be preferred. Therefore, using spectral values instead of time histories is preferred for the novel accidental eccentricity definition.

It can be seen from the figure that the structures with fundamental translational periods below 1.0 s are more prone to be affected by torsional ground motions. In the most extreme case—where b is 60 m, and γ is 1.5—the accidental eccentricity values may exceed 0.5. Any increase in parameters b and γ causes an increase in the implied accidental eccentricity, as was also observed in the previous section. However, the increase here emerges from the increasing inertial mass related to the torsional mode of vibration. When the b and γ parameters have larger values, the inertial mass of the torsional mode increases. Therefore, the required amount of torque to cause a certain rotation increases. Since the exerted translational force is constant, the accidental eccentricity coefficient needs to be larger to cause a larger torque. On the other hand, increasing values of the Ω parameter seem to enlarge the period range in which detrimental effects of the torsional ground motions are significant. The relatively larger values of accidental eccentricity coefficients are seen for periods below 0.5 s for the cases where Ω is 1.25. However, for the cases where Ω is 2.0, the relatively larger values can be seen for periods up to 1.4 s.

In the current practice, a design torsional ground motion or a torsional design spectrum is not available in most of the seismic design codes (ASCE 2021; TBEC 2018). To the best

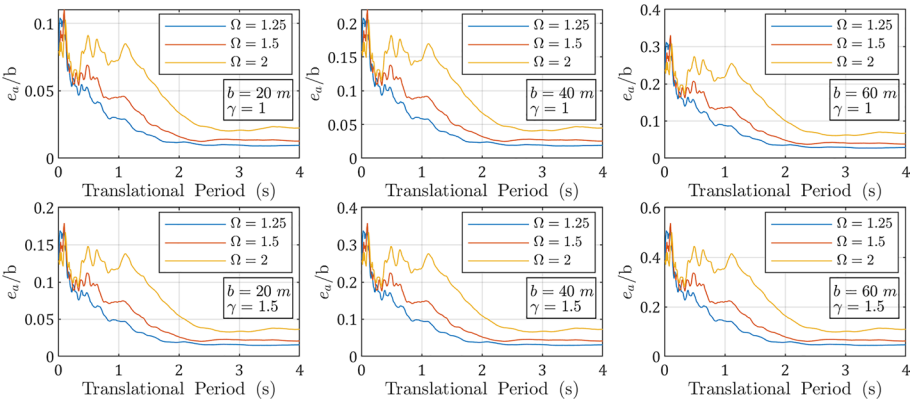

Fig. 12 Accidental eccentricity values obtained from the proposed procedure

of the authors' knowledge, only the Eurocode (1996) provides rotational spectra for the design of towers and masts. Eurocode (1996) provides rotational design spectra as a function of translational design spectra, based on the traveling wave approach (Newmark 1969). In Eurocode (1996), the relationship between translational and torsional design spectra is given as shown in Eq. 9. In Eq. 9, S_e corresponds to the translational acceleration spectrum, V_{S30} is the average shear wave velocity of the top 30 m of the soil site, T is the period, and R_z is the torsional acceleration spectrum. It must be noted that period T corresponds to the fundamental periods of both the torsional and translational vibration modes. Thus, it is implicitly assumed that the parameter Ω always equals unity.

$$R_z^{\theta}(T) = 2\pi \frac{S_e(T)}{V_{S,30}T} \tag{9}$$

After some manipulation, this equation can also be written in terms of the torsional rotation spectrum and translational acceleration spectrum as given in Eq. 10. In Eq. 10, SD^{tor} is the torsional rotation spectrum, and ω_θ is the angular frequency of the torsional fundamental mode of vibration.

$$SD^{tor}(T) = 2\pi \frac{S_e(T)}{V_{S,30}T\omega_\theta^2} \tag{10}$$

In Eq. 8, the accidental eccentricity coefficients are given as the multiplication of the response spectra ratio by some system parameters. Similarly, the ratio of Eurocode (1996) design spectra can be multiplied by the same system parameters to obtain implied accidental eccentricity coefficients as given in Eq. 11. The obtained accidental eccentricity coefficients can be used for bench-marking of the proposed procedure. Actually, the accidental eccentricity coefficients recommended by seismic codes are independent of the fundamental period. However, a comprehensive comparison of the accidental eccentricity coefficients can be achieved in this manner.

$$\frac{e_a}{b} = \frac{\pi b\left(1+\gamma^2\right)}{6TV_{S,30}} \tag{11}$$

As stated above, Eurocode (1996) assumes that the fundamental periods of torsional and translational modes of vibration are equal. Therefore, the accidental eccentricity values can only be determined for the cases where Ω equals to 1.0. On the other hand, in the previous section, it was stated that Ω values must satisfy the limit given in Eq. 3 to represent a realistic dynamic system. To satisfy this limitation, the γ value is set to 1.5, and a comparison of the accidental eccentricity coefficients is made by using these values.

The accidental eccentricity coefficients obtained by using Eurocode (1996) response spectra are given in comparison with the ones obtained by using the proposed procedure in Fig. 13. The Eurocode (1996) based accidental eccentricity values are truncated at period 0.1 s since the values go to infinity as the period approaches to 0. As seen from the figure, the Eurocode (1996) based accidental eccentricity values set an upper bound to the accidental eccentricity values obtained from the proposed procedure. It appears that the torsional response spectrum given in Eurocode (1996) is highly conservative. This is because the traveling wave velocity (i.e., phase velocity or apparent velocity) is assumed to be equal to $V_{S,30}$ in Eurocode (1996), which was shown to be inaccurate by Yin et al. (2016). It is also important to note that the Eurocode (1996)-based accidental eccentricity is proportional to $1/T$, whereas the proposed accidental eccentricity is proportional to $1/T^2$.

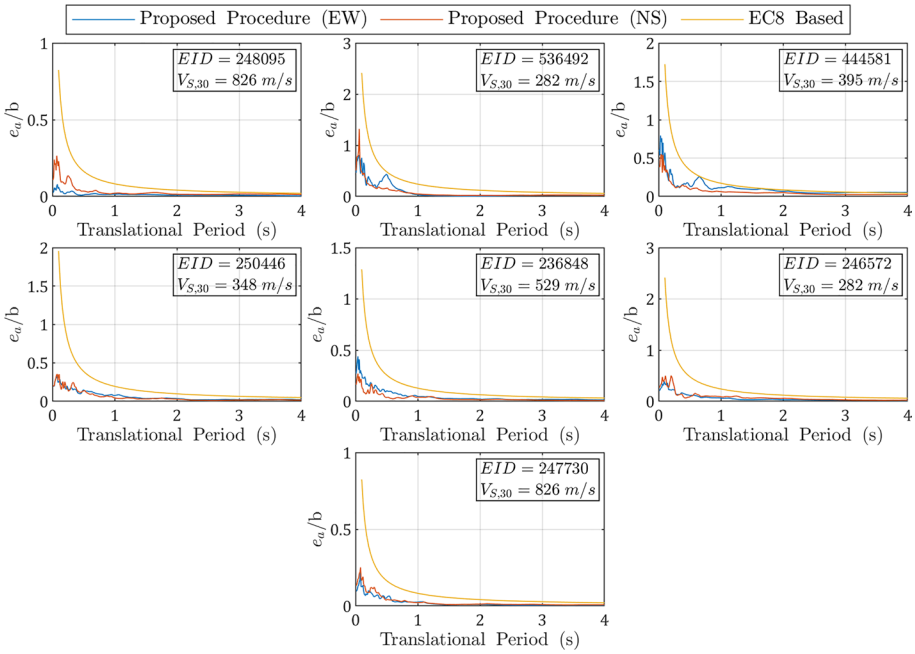

Fig. 13 Comparison of accidental eccentricities obtained from the proposed procedure with that derived from Eurocode (1996) response spectrum

Since this study utilizes regional seismic events that occurred in Turkey, the validity of the proposed accidental eccentricity coefficients is regional. If a large set of recordings together with site information were available, then a more general evaluation of the accidental eccentricity coefficients could be made. However, it appears that recommending accidental eccentricity coefficient spectra—rather than period-independent coefficients—would be the better approach. It should be noted here, however, that a specific spectra recommendation can/should only be made after a more comprehensive examination of regional seismic records than the limited exploration offered in the present study.

5 Conclusions

In seismic design codes, accidental eccentricity coefficients are recommended to be used to account for torsional ground motions. The recommended values are generally constant, such as 0.05 or 0.10. Although a number of studies have shown that these values are inadequate to account for torsional ground motions, there are still no updates on these values. On the other hand, it is also shown in the literature that the values of accidental eccentricity coefficients are period-dependent. However, a spectral representation for the accidental eccentricity coefficients is not available yet.

In this paper, seven seismic events that occurred in different regions of Turkey are employed to extract corresponding torsional ground motions. The corresponding accidental eccentricity coefficients for the obtained torsional ground motions are also determined. The conventional procedure is employed for calculating the corresponding

accidental eccentricity coefficients. However, the conventional procedure may yield negative accidental eccentricity coefficients depending on the ground motion time histories. Therefore, a more conservative approach is proposed for the determination of the corresponding accidental eccentricity coefficients. The proposed procedure yields accidental eccentricity coefficients which can exceed 0.5 in some cases, while they always have positive values. Additionally, using the proposed novel procedure, the accidental eccentricity values from the rotational design spectrum given in Eurocode (1996) Part 6 are also derived. Key findings are as follows:

- The accidental eccentricity coefficients proposed in Eurocode (1996) and TBEC (2018) could be unconservative for dynamic systems with smaller periods.
- The accidental eccentricity coefficients determined using the conventional approach may have negative values.
- The accidental eccentricity coefficients using the proposed approach will always be positive.
- The accidental eccentricity values are highly dependent on the fundamental period of the torsional vibration mode.
- Any increase in slab dimensions results in larger accidental eccentricity coefficients.
- The accidental eccentricity values implied by the torsional response spectra recommended in Eurocode (1996) Part 6 are significantly higher than those obtained in this study.

These findings obviously reveal a self-contradiction in the Eurocode (1996). On one hand, it recommends accidental eccentricity coefficients to be 0.05/0.10 for buildings, and on the other it defines a rotational design spectrum, which corresponds to very large accidental eccentricity coefficients. If the data-driven results from Turkey are to be trusted, then accidental eccentricity coefficients in Eurocode (1996) are too small (to account for torsional ground motions) while at the same time the accidental eccentricity coefficients implied by the rotational design spectra of Eurocode (1996) Part 6 are too large.

As stated before, there are a relatively limited number of seismic events employed in this study. Therefore, a comprehensive recommendation on accidental eccentricity values is not offered, which should be taken up in a future study. Synthetic records obtained from physics-based earthquake rupture simulations can also be used for detailed and direct examination of torsional ground motions in future studies, which can inform data-driven updating efforts on improving the accidental eccentricity coefficients provisioned in seismic codes.

Funding Open access funding provided by the Scientific and Technological Research Council of Türkiye (TÜBİTAK). This study was prepared during the first author's postdoctoral research at the University of California, Los Angeles, supported by The Scientific and Technological Research Council of Turkey (TUBITAK). Program code and name: 2219-International Postdoctoral Research Fellowship Program for Turkish Citizens.

Declarations

Competing interests The authors have no relevant financial or non-financial interests to disclose.

Open Access This article is licensed under a Creative Commons Attribution 4.0 International License, which permits use, sharing, adaptation, distribution and reproduction in any medium or format, as long as you give appropriate credit to the original author(s) and the source, provide a link to the Creative Commons licence, and indicate if changes were made. The images or other third party material in this article are included in the article's Creative Commons licence, unless indicated otherwise in a credit line to the material. If material is not included in the article's Creative Commons licence and your intended use is not permitted by statutory regulation or exceeds the permitted use, you will need to obtain permission directly from the copyright holder. To view a copy of this licence, visit http://creativecommons.org/licenses/by/4.0/.

References

AFAD (2022) Disaster and emergency management presidency strong ground motion database. Last Accessed 15 Dec 2022

Anagnostopoulos SA, Kyrkos MT, Stathopoulos KG (2015) Earthquake induced torsion in buildings: critical review and state of the art. Earthq Struct 8(2):305–377

ASCE-7 (2021) ASCE/SEI 7-22 Minimum Design Loads and Associated Criteria for Buildings and Other Structures. American Society of Civil Engineers (ASCE), USA

Basu D, Whittaker AS, Constantinou MC (2012) Estimating rotational components of ground motion using data recorded at a single station. J Eng Mech 138(9):1141–1156. https://doi.org/10.1061/(ASCE)EM.1943-7889.0000408

Basu D, Constantinou MC, Whittaker AS (2014) An equivalent accidental eccentricity to account for the effects of torsional ground motion on structures. Eng Struct 69:1–11. https://doi.org/10.1016/j.engstruct.2014.02.038

Dahmardeh SR, Motamedi M, Aziminejad A (2019) A study on the effects of torsional component of ground motions on seismic response of low- and mid-rise buildings. Struct Design Tall Spec Build. https://doi.org/10.1002/tal.1699

Eurocode-8 (1996) Eurocode 8: design provisions for earthquake resistance: Part 6: Towers, Masts, and Chimneys. BSI, London

Ghayamghamian MR, Nouri GR (2007) On the characteristics of ground motion rotational components using Chiba dense array data. Earthq Eng Struct Dyn 36(10):1407–1429. https://doi.org/10.1002/eqe.687

Ghayamghamian MR, Nouri GR, Igel H, Tobita T (2009) The effect of torsional ground motion on structural response: code recommendation for accidental eccentricity. Bull Seismol Soc Am 99(2B):1261–1270. https://doi.org/10.1785/0120080196

Gueguen P, Astorga A (2021) The torsional response of civil engineering structures during earthquake from an observational point of view. Sensors 21(2):342. https://doi.org/10.3390/s21020342

Housner GW, Outinen H (1958) The effect of torsional oscillations on earthquake stresses. Bull Seismol Soc Am 48(3):221–229

Mallet R (1846) On the dynamics of earthquakes; being an attempt to reduce their observed phenomena to the known laws of wave motion in solids and fluids. Trans R Irish Acad 21

Newmark NB (1969) Torsion in symmetrical buildings. In: Proceedings, Volume 2, Santiago, Chile. 4th World Conference on Earthquake Engineering, pp 19–32

Ozsahin E, Pekcan G (2019) Effect of torsional ground motion on the seismic response of highway bridges. Bull Earthq Eng 17(5):2603–2625. https://doi.org/10.1007/s10518-018-00550-8

Ozsahin E, Pekcan G (2020) Assessment of seismic demand due to torsional ground motions on symmetric skew bridges. J Earthq Eng 26(8):3938–3953. https://doi.org/10.1080/13632469.2020.1822224

Ozsahin E, Pekcan G (2020) Inelastic seismic response of box-girder bridges due to torsional ground motions. Eng Struct 218:110831. https://doi.org/10.1016/j.engstruct.2020.110831

Perron V, Hollender F, Mariscal A, Theodoulidis N, Andreou C, Bard PY, Cornou C, Cottereau R, Cushing EM, Frau A, Hok S, Konidaris A, Langlaude P, Laurendeau A, Savvaidis A, Svay A (2018) Accelerometer, velocimeter dense-array, and rotation sensor datasets from the sinaps@ postseismic survey (cephalonia 2014–2015 aftershock sequence). Seismol Res Lett 89(2A):678–687. https://doi.org/10.1785/0220170125

Poudel B, Ozsahin E, Pekcan G (2020) Effect of torsional ground motions on floor acceleration response in flexible SMRF buildings. J Earthq Eng 26(4):2168–2185. https://doi.org/10.1080/13632469.2020.1756990

Rutenberg A (1992) Nonlinear response of asymmetric building structures and seismic codes: a state of the art review. In: Fajfar P, Krawinkler H (eds) Nonlinear seismic analysis and design of reinforced concrete buildings, Chapter 23. CRC Press, London, pp 328–356

Rutenberg A, Heidebrecht AC (1985) Rotational ground motion and seismic codes. Can J Civ Eng 12(1):583–592

Spudich P, Steck LK, Hellweg M, Fletcher JB, Baker LM (1995) Transient stresses at parkfield, california, produced by the m 7.4 landers earthquake of June 28, 1992: Observations from the upsar dense seismograph array. J Geophys Res: Solid Earth 100(B1):675–690. https://doi.org/10.1029/94JB02477

TBEC-2018 (2018) Turkish Building and Earthquake Code. Disaster and Emergency Management Presidency (DEMP), Ankara

Yin J, Nigbor RL, Chen Q, Steidl J (2016) Engineering analysis of measured rotational ground motions at gvda. Soil Dyn Earthq Eng 87:125–137. https://doi.org/10.1016/j.soildyn.2016.05.007

Publisher's Note Springer Nature remains neutral with regard to jurisdictional claims in published maps and institutional affiliations.

Authors and Affiliations

Rafet Sisman[1,2] · Ertugrul Taciroglu[2]

✉ Rafet Sisman
rafet@yildiz.edu.tr

Ertugrul Taciroglu
etacir@g.ucla.edu

[1] Department of Civil Engineering, Yildiz Technical University, Davutpasa Campus, Esenler, 34420 Istanbul, Turkey

[2] Department of Civil and Environmental Engineering, University of California Los Angeles, 5731 Boelter Hall, Los Angeles, CA 90095, US